

Analytical Models for the Estimation of Effect of the Spray Angle on a Subcooled Target

Arun V Rejus Kumar and A. Sagai Francis Britto

Abstract--- Since its beginnings nearly a century ago, plant superintendents and maintenance personnel have relied on thermal spray technology as a cost-effective means to repair worn components and incorrectly machined parts for light and heavy industrial equipment. The manufactures of thermal spray equipment and materials have continued their efforts to make thermal spray technology more attractive by creating new spray systems and materials. As a result, it is now possible to tailor a coating solution to fit a customer's needs. Thermal sprayed coatings are used extensively for a wide range of industrial applications. The technique generally involves the spraying of molten powder or wire feedstock, the melting technique achieved by oxy-fuel combustion or an electric arc (plasma). The molten particles are accelerated by the flame, followed by impacting onto a properly prepared substrate, usually metallic. Solidification occurs at rates akin to those obtained in Rapid Solidification Technology. Thus, the as-sprayed deposit is ultra-fine grained. Having the properties associated with such microstructures. The materials which are sprayed include most metal alloys and ceramics. In fact, virtually any material can be thermal sprayed as long as it does to decompose prior to melting. In this paper, we present a simple analytical mathematical model for the estimation of the maximum splat diameter of an impacting droplet on a subcooled target. The model uses an energy conservation argument, applied between the initial and final drop configurations, to approximately capture the dynamics of spreading. The effects of viscous dissipation, surface tension, and contact angle are taken into account. Tests against limited experimental data at high Reynolds and Weber numbers indicate that accuracy of the order of 5% is achieved. Also the effect of the spray angle on the maximum splat diameter can be calculated. Thus once the maximum splat diameter is found the thermal spraying process can be optimized for maximum efficiency. Various parameters like the initial droplet velocity, contact angle etc. can be pre-determined, thus making the process cost-efficient.

Keywords--- Analytical Models, Spray Angle, Subcooled Target, Pre-determined.

I. INTRODUCTION

In recent years various simple analytical models for the estimation of the maximum splat diameter of an impacting droplet on a subcooled target have been proposed. Such models could prove very useful as preliminary design tools in the rapidly developing field of microfabrication. They can additionally facilitate the understanding of the couple droplet spreading and solidification dynamics, which will lead to improvement in microfabrication quality. In this paper we present a model that accounts for the effects of surface tension, contact angle, and solidification at the droplet-target interface.

Arun V Rejus Kumar, Assistant Professor, Department of Mechanical Engineering, BIST, BIHER, Bharath Institute of Higher Education & Research, Selaiyur, Chennai.

A. Sagai Francis Britto, Research Scholar, DST- JRF (INSPIRE Fellow), Department of Mechanical Engineering, BIST, BIHER, Bharath Institute of Higher Education & Research, Selaiyur, Chennai.

Consider a superheated liquid metal droplet of diameter D_o and at temperature $T_o > T_m$ impacting a subcooled solid substrate (temperature $T_w < T_m$) with velocity V_o . We are interested in the limit of small superheat, that is $(T_o - T_m) \rightarrow 0$ where T_m is the melting temperature. When spreading stops, the droplet has reached the maximum splat configuration in the shape of a thin disk of diameter D , and height h . We assume that the material has partially solidified: a thin layer of thickness s (averaged over the diameter) at the substrate-droplet interface is now solid at (an average) temperature T , where $T_w < T < T_o$, and the remaining droplet material is molten at T_m . The maximum splat ratio ξ is defined as $\xi = D_m/D_o$. One important assumption used in this work is that the droplet arrest is not governed by solidification, that is the effect of heat transfer and solidification is only secondary to the spread process.

In the isothermal case the target and droplet are at the same temperature ($T_o = T_w$) and negligible heat exchange takes place between the two.

II. THE MAXIMUM SPLAT DIAMETER

The maximum spread diameter, D_m can be estimated by using an energy conservation argument: the energy at every instant in time, and hence at the maximum splat diameter configuration (configuration 2), has to equal the initial energy of the drop (configuration 1). This initial energy is equal to the sum of the kinetic energy (KE_1) and the surface energy (SE_1) of the impacting droplet. The kinetic energy is given by:

$$KE_1 = \left(\frac{1}{2} \rho V_o^2 \right) \left(\frac{1}{6} \pi D_o^3 \right)$$

Where ρ is the liquid drop density. The initial surface energy is given by:

$$SE_1 = \pi D_o^2 \gamma$$

Where γ (gamma) is the surface tension coefficient for the drop in the ambient environment. The energy at the maximum splat configuration consists of the energy dissipated through the action of viscosity during the spreading process and the surface energy of the maximum splat configuration. The first term has been shown (Pasandideh-Fard et al., 1996) to (approximately) equal.

$$W = \frac{\pi}{3} \rho V_o^2 D_o D_m^2 \frac{1}{\sqrt{R_e}}$$

Where, $R_e = \rho V_o D_o / \mu$ is the Reynolds's number. This estimate is obtained by assuming an axisymmetric stagnation point flow which in the high Reynold limit can be approximated by a viscous boundary layer of thickness $\delta = 2D_o / \sqrt{R_e}$ and potential flow outside this boundary layer.

The surface energy (SE_2) is estimated by assuming that the final configuration approximates a thin disk. It is shown by Collings et al. (1989) that given the contact angle (θ_a), and the disk-shape geometry assumption with diameter D_m , and height h that is small compared to D_m

$$SE_2 = \frac{\pi}{4} D_m^2 \gamma (1 - \cos \theta_a)$$

Equating,

$$KE_1 + SE_1 = W + SE_2$$

Substituting the values,

$$\left(\frac{1}{2} \rho V_o^2 \right) \left(\frac{1}{6} \pi D_o^3 \right) + \pi D_o^2 \gamma = \frac{\pi}{3} \rho V_o^2 D_o D_m^2 \frac{1}{\sqrt{R_e}} + \frac{\pi}{4} D_m^2 \gamma (1 - \cos \theta_a)$$

$$D_m = D_o \sqrt{\frac{\frac{\rho V_o^2 D_o}{12} + \gamma}{\frac{\rho V_o^2 D_o}{3\sqrt{R_e}} + \frac{\gamma(1 - \cos \theta)}{4}}}$$

Where V_o is equal to V_N in our case.

Assuming initial droplet velocity to be constant we get a relation between:

- ▶▶ Maximum splat diameter (D_m)
- ▶▶ Initial droplet diameter (D_o)
- ▶▶ Contact angle (θ_a)

III. RESULTS

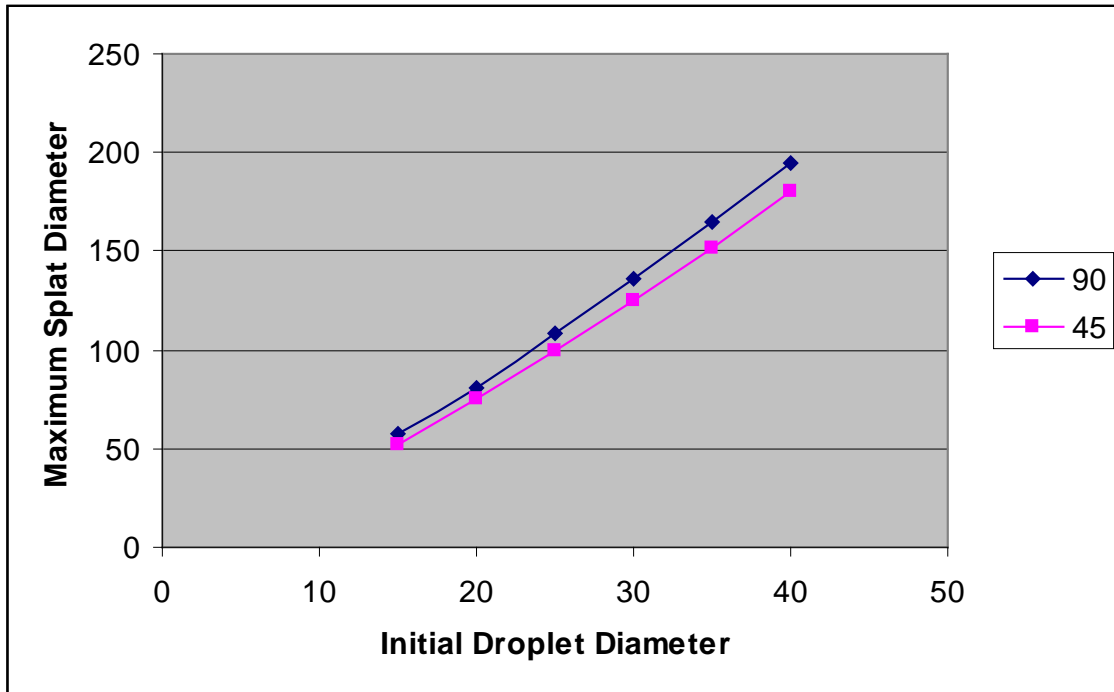
- Tin and Stainless Steel were used in the simulation. The impinging droplet was of Tin (Sn) and the substrate was made up of Stainless Steel.
- The properties for Tin and Stainless Steel are given below:

Droplet Initial Temperature:	519 K
Substrate Initial Temperature:	298 K
Solidus Temperature:	504 K
Liquidus Temperature:	506 K
Thermal conductivity of solid tin:	33.6 W(mK) ⁻¹
Thermal conductivity of liquid tin:	62.2 W(mK) ⁻¹
Thermal conductivity of Steel:	14.9 W(mK) ⁻¹
Density of Steel:	7900 kg m ⁻³

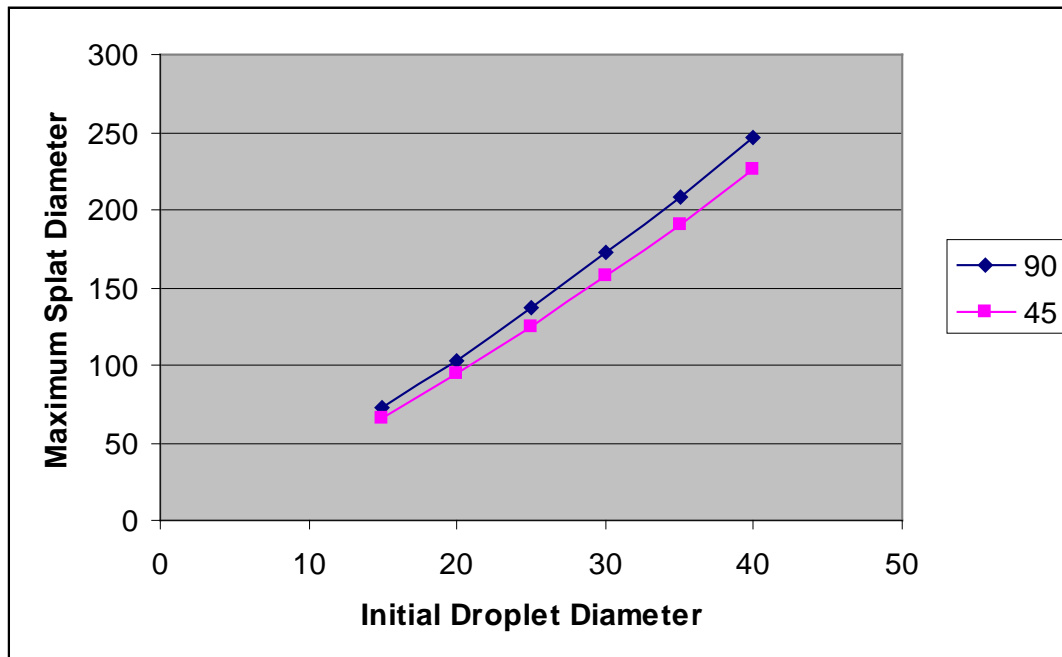
Density of liquid tin:	6980 kg m ⁻³
Density of solid tin:	7200 kg m ⁻³
Droplet surface tension:	0.566 N m ⁻¹
Specific heat of droplet:	244 J(kg K) ⁻¹
Specific heat of Steel:	477 J(kg K) ⁻¹
Viscosity of liquid Tin:	3 × 10 ⁻³ N.s m ⁻¹
Latent heat of solidification:	58500 J kg ⁻¹

<i>Initial Droplet Diameter</i> $D_o (\mu m)$	<i>Initial Velocity</i> V_o (m/s)	<i>Contact Angle</i> θ_a	<i>Normal Velocity</i> $V_N = V_o \cos \theta$	<i>Reynolds no.</i> Re_N	<i>Maximum Diameter</i> $D_m (\mu m)$	<i>Splat</i>
15	100	90	100	3490	57	
20	100	90	100	4653	81	
25	100	90	100	5816	108	
30	100	90	100	6980	136	
35	100	90	100	8143	165	
40	100	90	100	9306	195	
15	100	45	70.71	2467	52	
20	100	45	70.71	3290	75	
25	100	45	70.71	4112	100	
30	100	45	70.71	4935	125	
35	100	45	70.71	5758	152	
40	100	45	70.71	6580	180	
15	250	90	250	8725	72	
20	250	90	250	11633	103	
25	250	90	250	14541	137	
30	250	90	250	17450	172	
35	250	90	250	20358	208	
40	250	90	250	23266	246	
15	250	45	176.77	6169	66	
20	250	45	176.77	8225	95	
25	250	45	176.77	10282	125	
30	250	45	176.77	12338	158	
35	250	45	176.77	14394	191	
40	250	45	176.77	16451	226	

Impact Velocity 100 m/s

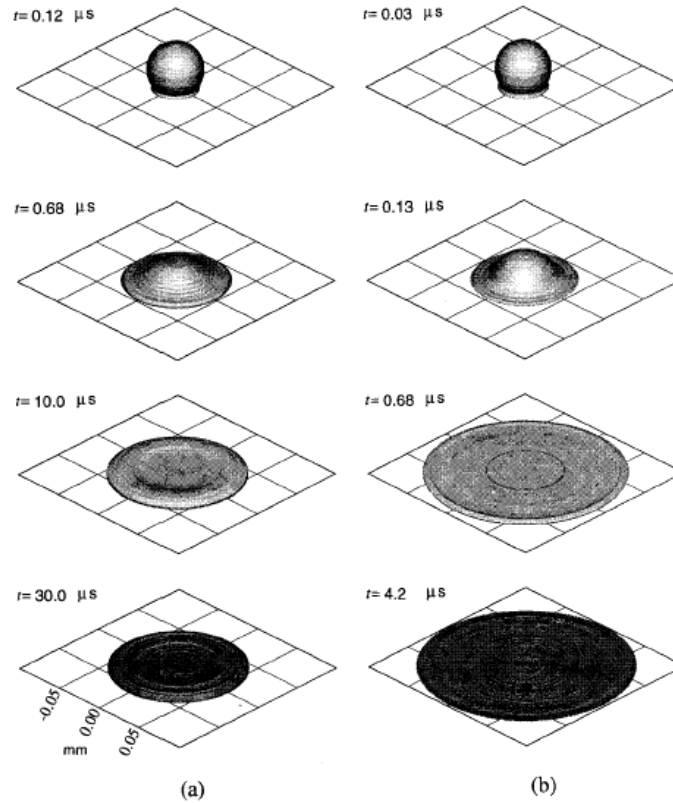


Impact Velocity 250 m/s

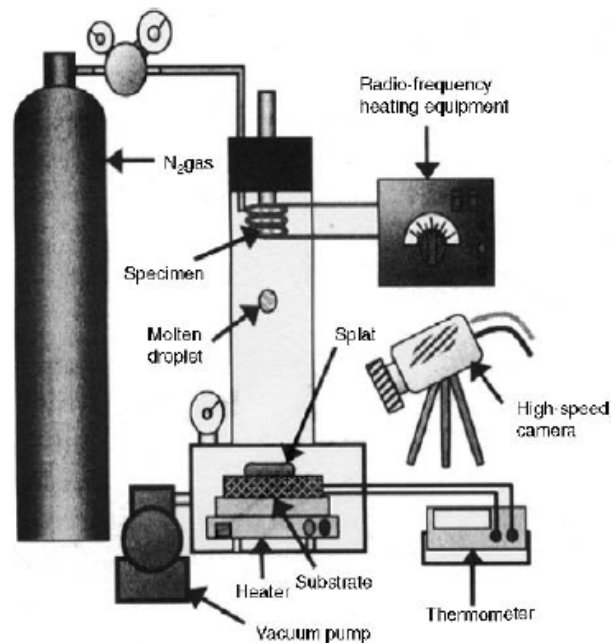


IV. SPLAT FORMATION PROCESS

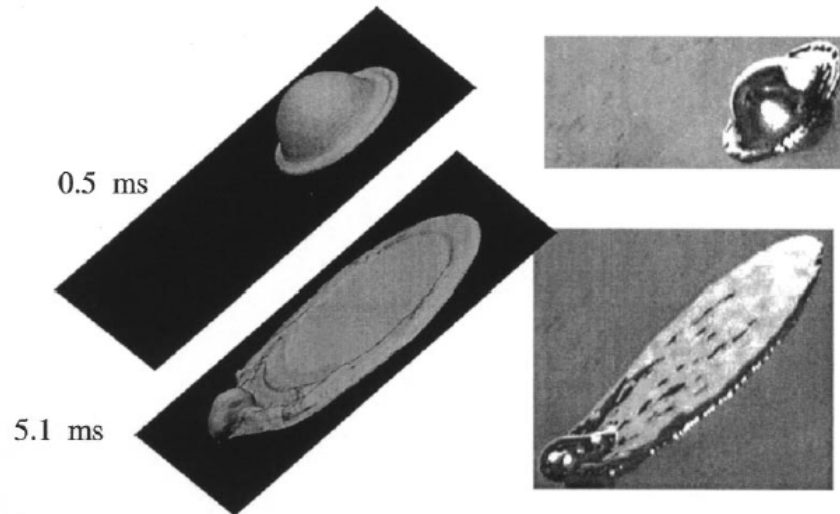
Predicted Sequence of deformation and solidification for the tin droplet impinging on the steel substrate.



Predicted sequence of deformation and solidification for the alumina droplet; 50 μm diameter; 246°C initial temperature; 90 degrees contact angle; no contact resistance; (a) 100 m / s impact velocity; (b) 250 m/s impact velocity.



Schematic drawing of the experimental setup to study the impact of a millimeter-sized particle



Comparison of the predicted (left column) and photographs (right column) of the impact of tin droplet on stainless steel substrate. Droplet diameter 2.2 mm; impact speed 100 m/s; initial drop temperature 246 °C; initial substrate temperature 25 °C; incline angle 45°.

REFERENCES

- [1] Thooyamani, K.P., Khanaa, V., & Udayakumar, R. (2014). Virtual instrumentation based process of agriculture by automation. *Middle-East Journal of Scientific Research*, 20(12): 2604-2612.
- [2] Udayakumar, R., Kaliyamurthie, K.P., & Khanaa, T.K. (2014). Data mining a boon: Predictive system for university topper women in academia. *World Applied Sciences Journal*, 29(14): 86-90.
- [3] Anbuselvi, S., Rebecca, L.J., Kumar, M.S., & Senthilvelan, T. (2012). GC-MS study of phytochemicals in black gram using two different organic manures. *J Chem Pharm Res.*, 4, 1246-1250.
- [4] Subramanian, A.P., Jaganathan, S.K., Manikandan, A., Pandiaraj, K.N., Gomathi, N., & Supriyanto, E. (2016). Recent trends in nano-based drug delivery systems for efficient delivery of phytochemicals in chemotherapy. *RSC Advances*, 6(54), 48294-48314.
- [5] Thooyamani, K.P., Khanaa, V., & Udayakumar, R. (2014). Partial encryption and partial inference control based disclosure in effective cost cloud. *Middle-East Journal of Scientific Research*, 20(12), 2456-2459.
- [6] Lingeswaran, K., Prasad Karamcheti, S.S., Gopikrishnan, M., & Ramu, G. (2014). Preparation and characterization of chemical bath deposited cds thin film for solar cell. *Middle-East Journal of Scientific Research*, 20(7), 812-814.
- [7] Maruthamani, D., Vadivel, S., Kumaravel, M., Saravanakumar, B., Paul, B., Dhar, S.S., Manikandan, A., & Ramadoss, G. (2017). Fine cutting edge shaped Bi₂O₃rods/reduced graphene oxide (RGO) composite for supercapacitor and visible-light photocatalytic applications. *Journal of colloid and interface science*, 498, 449-459.
- [8] Gopalakrishnan, K., Sundeep Aanand, J., & Udayakumar, R. (2014). Electrical properties of doped azopolyester. *Middle-East Journal of Scientific Research*, 20(11). 1402-1412.
- [9] Subhashree, A.R., Parameaswari, P.J., Shanthi, B., Revathy, C., & Parijatham, B.O. (2012). The reference intervals for the haematological parameters in healthy adult population of chennai, southern India. *Journal of Clinical and Diagnostic Research: JCDR*, 6(10), 1675-1680.
- [10] Niranjana, U., Subramanyam, R.B.V., & Khanaa, V. (2010, September). Developing a web recommendation system based on closed sequential patterns. In *International Conference on Advances in Information and Communication Technologies*, 101, 171-179. Springer, Berlin, Heidelberg.
- [11] Slimani, Y., Baykal, A., & Manikandan, A. (2018). Effect of Cr³⁺ substitution on AC susceptibility of Ba hexaferrite nanoparticles. *Journal of Magnetism and Magnetic Materials*, 458, 204-212.
- [12] Premkumar, S., Ramu, G., Gunasekaran, S., & Baskar, D. (2014). Solar industrial process heating associated with thermal energy storage for feed water heating. *Middle East Journal of Scientific Research*, 20(11), 1686-1688.

- [13] Kumar, S.S., Karrunakaran, C.M., Rao, M.R.K., & Balasubramanian, M.P. (2011). Inhibitory effects of *Indigofera aspalathoides* on 20-methylcholanthrene-induced chemical carcinogenesis in rats. *Journal of carcinogenesis*, 10.
- [14] Beula Devamalar, P.M., Thulasi Bai, V., & Srivatsa, S.K. (2009). Design and architecture of real time web-centric tele health diabetes diagnosis expert system. *International Journal of Medical Engineering and Informatics*, 1(3), 307-317.
- [15] Ravichandran, A.T., Srinivas, J., Karthick, R., Manikandan, A., & Baykal, A. (2018). Facile combustion synthesis, structural, morphological, optical and antibacterial studies of Bi_{1-x}Al_xFeO₃ (0.0 ≤ x ≤ 0.15) nanoparticles. *Ceramics International*, 44(11), 13247-13252.
- [16] Thovhogi, N., Park, E., Manikandan, E., Maaza, M., & Gurib-Fakim, A. (2016). Physical properties of CdO nanoparticles synthesized by green chemistry via Hibiscus Sabdariffa flower extract. *Journal of Alloys and Compounds*, 655, 314-320.
- [17] Thooyamani, K.P., Khanaa, V., & Udayakumar, R. (2014). Wide area wireless networks-IETF. *Middle-East Journal of Scientific Research*, 20(12), 2042-2046.
- [18] Sundar Raj, M., Saravanan, T., & Srinivasan, V. (2014). Design of silicon-carbide based cascaded multilevel inverter. *Middle-East Journal of Scientific Research*, 20(12), 1785- 1791.
- [19] Achudhan, M., Jayakumar M.P. (2014). Mathematical modeling and control of an electrically-heated catalyst. *International Journal of Applied Engineering Research*, 9(23), 23013.
- [20] Thooyamani, K.P., Khanaa, V., & Udayakumar, R. (2013). Application of pattern recognition for farsi license plate recognition. *Middle-East Journal of Scientific Research*, 18(12), 1768-1774.
- [21] Jebaraj, S., Iniyani S. (2006). Renewable energy programmes in India. *International Journal of Global Energy Issues*, 26(43528), 232-257.
- [22] Sharmila, S., & Jeyanthi Rebecca, L. (2013). Md Saduzzaman., Biodegradation of domestic effluent using different solvent extracts of *Murraya koenigii*. *J Chem and Pharm Res*, 5(2), 279-282.
- [23] Asiri, S., Sertkol, M., Guner, S., Gungunes, H., Batoo, K.M., Saleh, T.A., Manikandan A., & Baykal, A. (2018). Hydrothermal synthesis of CoyZnyMn1-2yFe2O4 nanoferrites: magneto-optical investigation. *Ceramics International*, 44(5), 5751-5759.
- [24] Rani, A.J., & Mythili, S.V. (2014). Study on total antioxidant status in relation to oxidative stress in type 2 diabetes mellitus. *Journal of clinical and diagnostic research: JCDR*, 8(3), 108-110.
- [25] Karthik, B. (2014). Arulselvi, Noise removal using mixtures of projected gaussian scale mixtures. *Middle-East Journal of Scientific Research*, 20(12), 2335-2340.
- [26] Karthik, B., Arulselvi, & Selvaraj, A. (2014). Test data compression architecture for low power VLSI testing. *Middle - East Journal of Scientific Research*, 20(12), 2331-2334.
- [27] Vijayaragavan, S.P., Karthik, B., & Kiran Kumar, T.V.U. (2014). Privacy conscious screening framework for frequently moving objects. *Middle-East Journal of Scientific Research*, 20(8), 1000-1005.
- [28] Kaliyamurthie, K.P., Parameswari, D., & Udayakumar, R. (2013). QOS aware privacy preserving location monitoring in wireless sensor network. *Indian Journal of Science and Technology*, 6(5), 4648-4652.
- [29] Silambarasu, A., Manikandan, A., & Balakrishnan, K. (2017). Room-temperature superparamagnetism and enhanced photocatalytic activity of magnetically reusable spinel ZnFe₂O₄ nanocatalysts. *Journal of Superconductivity and Novel Magnetism*, 30(9), 2631-2640.
- [30] Jasmin, M., Vigneshwaran, T., & Beulah Hemalatha, S. (2015). Design of power aware on chip embedded memory based FSM encoding in FPGA. *International Journal of Applied Engineering Research*, 10(2), 4487-4496.
- [31] Philomina, S., & Karthik, B. (2014). Wi-Fi energy meter implementation using embedded linux in ARM 9. *Middle-East Journal of Scientific Research*, 20, 2434-2438.
- [32] Vijayaragavan, S.P., Karthik, B., & Kiran Kumar, T.V.U. (2014). A DFIG based wind generation system with unbalanced stator and grid condition. *Middle-East Journal of Scientific Research*, 20(8), 913-917.
- [33] Rajakumari, S.B., & Nalini, C. (2014). An efficient data mining dataset preparation using aggregation in relational database. *Indian Journal of Science and Technology*, 7, 44-46.
- [34] Karthik, B., Kiran Kumar, T.V.U., Vijayaragavan, P., & Bharath Kumaran, E. (2013). Design of a digital PLL using 0.35 μm CMOS technology. *Middle-East Journal of Scientific Research*, 18(12), 1803-1806.
- [35] Sudhakara, P., Jagadeesh, D., Wang, Y., Prasad, C.V., Devi, A.K., Balakrishnan, G., Kim B.S., & Song, J.I. (2013). Fabrication of Borassus fruit lignocellulose fiber/PP composites and comparison with jute, sisal and coir fibers. *Carbohydrate polymers*, 98(1), 1002-1010.
- [36] Kanniga, E., & Sundararajan, M. (2011). Modelling and characterization of DCO using pass transistors. In *Future Intelligent Information Systems*, 86(1), 451-457. Springer, Berlin, Heidelberg.

- [37] Sachithanandam, P., Meikandaan, T.P., & Srividya, T. Steel framed multi storey residential building analysis and design. *International Journal of Applied Engineering Research*, 9(22), 5527-5529.
- [38] Kaliyamurthie, K.P., Udayakumar, R., Parameswari, D., & Mugunthan, S.N. (2013). Highly secured online voting system over network. *Indian Journal of Science and Technology*, 6(S6), 4831-4836.
- [39] Sathyaseelan, B., Manikandan, E., Lakshmanan, V., Baskaran, I., Sivakumar, K., Lachchumananandasivam, R., Kennedy, J., & Maaza, M. (2016). Structural, optical and morphological properties of post-growth calcined TiO₂ nanopowder for opto-electronic device application: Ex-situ studies. *Journal of Alloys and Compounds*, 671, 486-492.
- [40] Saravanan, T., Sundar Raj M., & Gopalakrishnan K. (2014). SMES technology, SMES and facts system, applications, advantages and technical limitations. *Middle - East Journal of Scientific Research*, 20(11), 1353-1358.
- [41] Ristono, A., & Budi, P. (2019). Design of Reliable and Efficient Manchester Carry Chain Adder based 8-BIT ALU for High Speed Applications. *Journal of VLSI Circuits And Systems*, 1(1), 1-4.
- [42] Anoop, T.R., & Mini, M.G. (2015). Altered Fingerprint Matching Using Ridge Texture and Frequency in the Unaltered Region. *Bonfring International Journal of Advances in Image Processing*, 5(2), 06-09.
- [43] Sindhuja, R. (2019). An Analysis of Image Segmentation techniques. *Journal of Computational Information Systems*, 15(1), 171-175.
- [44] Sudarsanam, P. (2019). Location Oriented Android Discount Tracker. *Journal of Computational Information Systems*, 15(2), 15-21.
- [45] Sharma, D.K. (2019). Performance Evaluation of SFIG and DFIG Based Wind Turbines. *Journal of Computational Information Systems*, 15(2), 45-53.
- [46] Nemmani, D.S. (2019). SCADA System Application for Power Distribution in Hyderabad City. *Journal of Computational Information Systems*, 15(3), 79-88.
- [47] Gireesha. B. (2018). A Comparative Performance Evaluation of Swarm Intelligence Techniques *Journal of Computational Information Systems*, 14(4), 14 - 20.
- [48] Santhanaraj, M., Prasanth, S., Sarath Kumar, K., Vishnu Chander, R., & Vijayaragavan, T. (2015). Segmentation and Detection of Magnetic Resonance Image Based on K-Mean Algorithm. *International Journal of Advances in Engineering and Emerging Technology*, 7(3), 133-138.
- [49] Eswari, K.E., and Arunkumar, R.K. (2014). Wi-Fi Technology. *Excel International Journal of Technology, Engineering and Management*, 1(2), 42-45.
- [50] Job, D., & Paul, V. (2016). Recursive Backtracking for Solving 9*9 Sudoku Puzzle. *Bonfring International Journal of Data Mining*, 6(1), 07-09.